SHINGLE OF A ROOF – CU ALLOY – MODERN TIMES – SWITZERLAND

Artefact name	Shingle of a roof
Authors	Marianne. Senn (EMPA, Dübendorf, Zurich, Switzerland) & Christian. Degrigny (HE-Arc CR, Neuchâtel, Neuchâtel, Switzerland)
Url	/artefacts/318/

The object

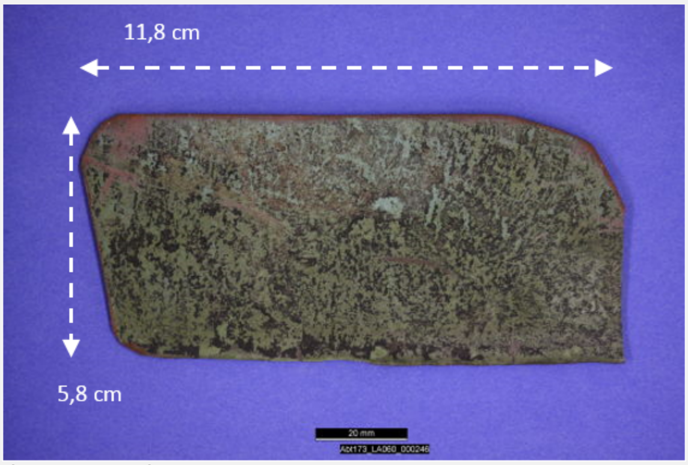

Credit HE-Arc CR.

Fig. 1: Copper alloy shingle, internal side,

Description and visual observation

Description of the artefact	Shingle, slightly curved, the internal side is covered with heterogeneously distributed green and black corrosion products (Fig. 1). The external side shows a regular dark green corrosion crust. Dimensions: L = 11.8cm; W = 5.8cm.
Type of artefact	Architectural element
Origin	Roof of the Abbey of St Gallen, Sankt Gallen, Saint Gallen, Switzerland
Recovering date	None
Chronology category	Modern Times
chronology tpq	1780 A.D.
chronology taq	----
Chronology comment	1780
Burial conditions / environment	Outdoor atmosphere
Artefact location	Conservation Department of the Musées d'art et d'histoire, Genève, Geneva
Owner	Abbey of St Gallen, Sankt Gallen, Saint Gallen

Inv. number None

Recorded conservation data Not conserved

Complementary information

Nothing to report.

Study area(s)

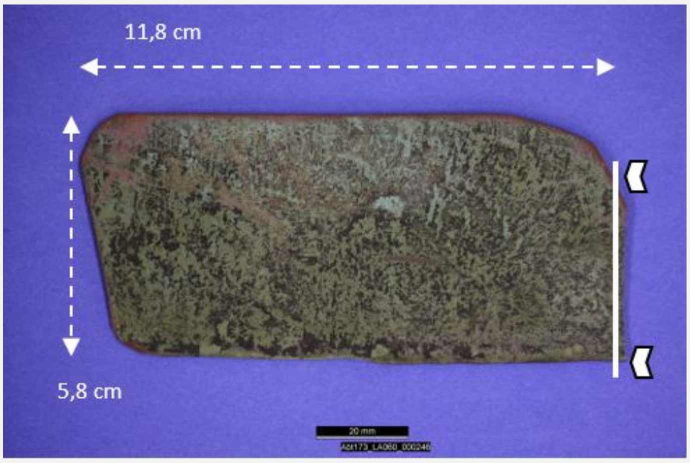

Credit HE-Arc CR.

Fig. 2: showing the location of sampling area,

Binocular observation and representation of the corrosion structure

Stratigraphic representation: none.

MiCorr stratigraphy(ies) – Bi

Sample(s)

Fig. 3: Micrograph of the cross-sections showing the location of Figs. 5 to 8,

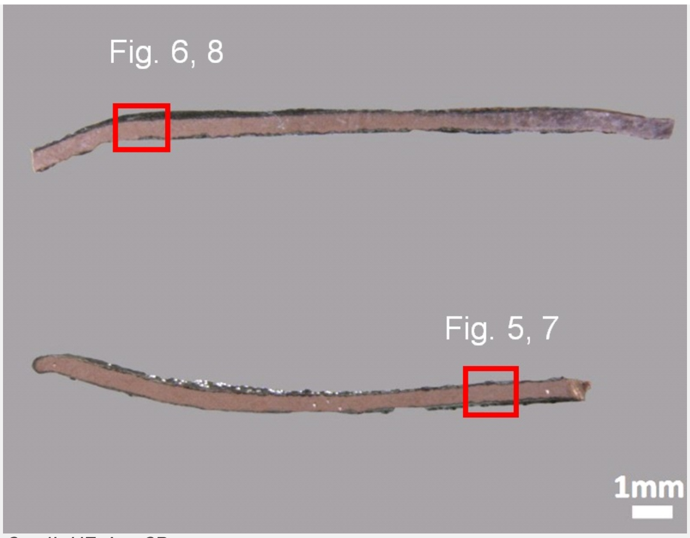

Credit HE-Arc CR.

Description of sample	Two samples were taken (Fig. 2). The polished samples show a well-preserved metal surface with a thin corrosion crust (Fig. 3). T = 0.5mm.
Alloy	Cu Alloy
Technology	Rolled (probably hot rolling) and annealed
Lab number of sample	MAH-98-257
Sample location	Empa (Marianne Senn)
Responsible institution	Conservation Department of the Musées d'art et d'histoire, Genève, Geneva
Date and aim of sampling	2009, integration of sample to the MIFAC-Métal project

Complementary information

Nothing to report.

Analyses and results

Analyses performed:
Metallography (etched with ferric chloride reagent), Vickers hardness testing, LA-ICP-MS, SEM/EDS, XRD, Raman spectroscopy.

Non invasive analysis

Metal

The remaining metal is a copper alloy (Table 1). The evenly distributed inclusions observed under SEM, SE-mode, are either light-grey or white (Fig. 5). The oval shape of the light-grey inclusions is due to deformation, probably by hot rolling (a common technique in the 18th century). Under polarised light they look red (Fig. 7) and their analysis reveals a composition similar to cuprite/Cu_2O (Table 2). The white inclusions are rich in Pb and are remnants of the refining process (Table 2). The etched copper shows a structure of polygonal and twinned grains (Fig. 6). The grain size is variable. The average hardness of the metal is about HV1 70.

Elements	Cu	Pb	As	Sb	Ag	Bi	Sn	Zn	Ni	Fe	Co
mass%	99	0.7	0.1	0.1	0.05	<	<	<	<	<	<
RSD %	0.3	25	20	7	4						

Table 1: Chemical composition of the metal. Method of analysis: LA-ICP-MS, Laboratory of Basic Aspects of Analytical Chemistry at the Faculty of Chemistry, University of Warsaw, PL.

Elements	O	Cu	Pb	As	Sb	Total
Light-grey inclusion	9.8	86	<	<	<	96
White inclusion	9	9.1	68	5.1	2.6	94

Table 2: Chemical composition (mass %) of the inclusions in the metal (from Fig. 5). Method of analysis: SEM/EDS, Laboratory of Analytical Chemistry, Empa.

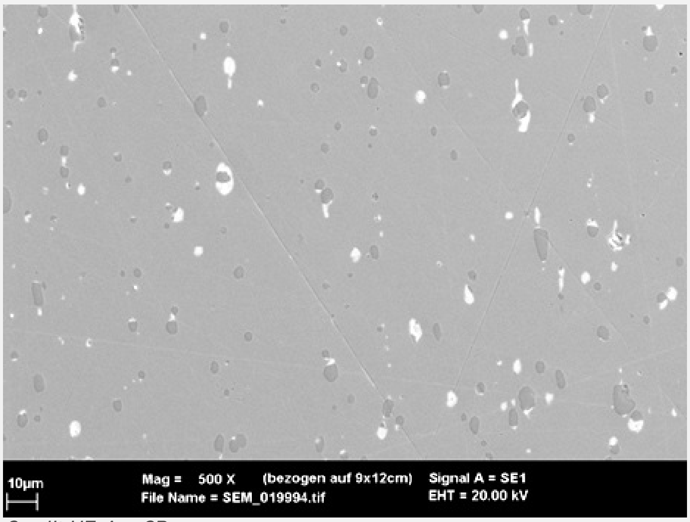

Credit HE-Arc CR.

Fig. 5: SEM image, SE-mode, of the metal sample from Fig. 3 (detail). Light-grey and white inclusions are distributed evenly,

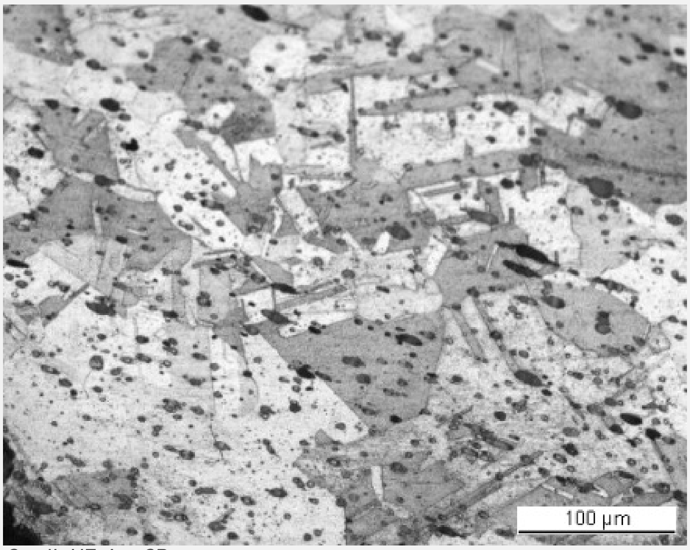

Credit HE-Arc CR.

Fig. 6: Micrograph of the metal sample from Fig. 3 (detail), etched, bright field. The metal shows a structure of polygonal and twinned grains. Cuprite inclusions appear as dark spots,

Microstructure Polygonal and twinned grains, elongated inclusions

First metal element Cu

Other metal elements

Complementary information

Nothing to report.

Corrosion layers

The corrosion crusts of the external and internal sides are distinctively different (Fig. 7). On the internal side an irregular red-orange corrosion layer has developed, and pitting corrosion has occurred. The more uniform corrosion layers on the external side are composed of a red-orange layer, followed by a thicker green outer layer. In some areas, dark-red corrosion products can be observed between the green and red-orange sub-layers. The same dark-red sub-layer can be seen in areas on the internal side covering the red-orange corrosion products. The red-orange corrosion layer on both sides (CP2) has a chemical composition similar to cuprite/Cu_2O, while the green layer on the external side (CP1) contains Cu, S and O and is enriched on its upper surface with Si (Table 3 and Fig. 8). XRD analysis of the corrosion products on the external side of another shingle fragment from the same roof identified brochantite/$Cu_4SO_4(OH)_6$ and cuprite as corrosion products (Rapport d'analyse no. MAH 98-257). These results are confirmed by Raman spectroscopy of the external side of this sample where the same compounds were clearly identified (Figs. 9 and 10).

Elements	O	Cu	S	Total
CP1	20	59	6.2	85
CP2	11	86	<	97

Table 3: Chemical composition (mass %) of the corrosion layers of the external side. Method of analysis: SEM/EDS, Laboratory of Analytical Chemistry, Empa.

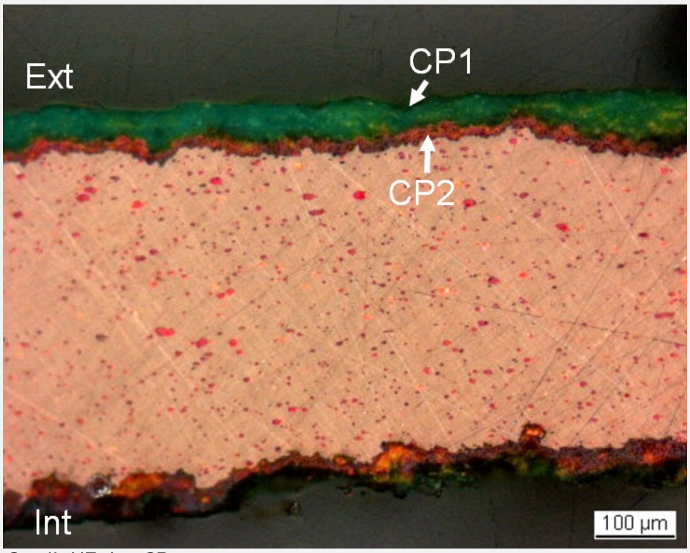

Credit HE-Arc CR.

Fig. 7: Micrograph of the metal sample from Fig. 3 and corresponding to the stratigraphy of Fig. 4, polarised light. External side: the regular corrosion crust with outer green, inner red-orange corrosion products and intermediate dark-red corrosion products. Internal side: the irregular corrosion crust with inner red-orange and outer dark-red corrosion products,

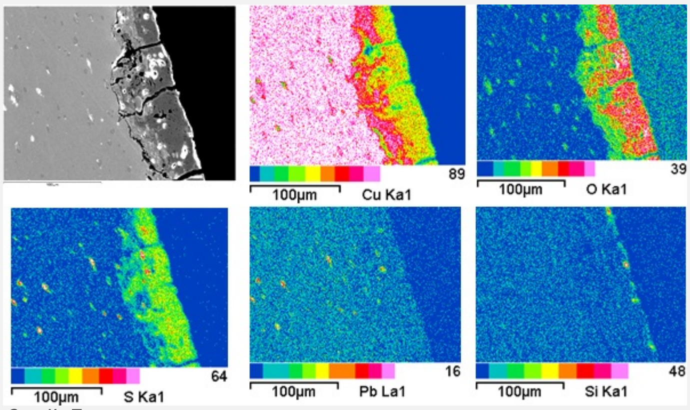

Credit Empa.

Fig. 8: SEM image, SE-mode, and elemental chemical distribution of the selected area of Fig. 3 (rotated image, detail). Method of examination: SEM/EDS, Laboratory of Analytical Chemistry, Empa,

Fig. 9: Raman spectrum of the red-orange inner corrosion layer (CP2) of the external side (cat3_B) compared to a cuprite standard spectrum. Settings: laser wavelength 532nm, acquisition time 100s,

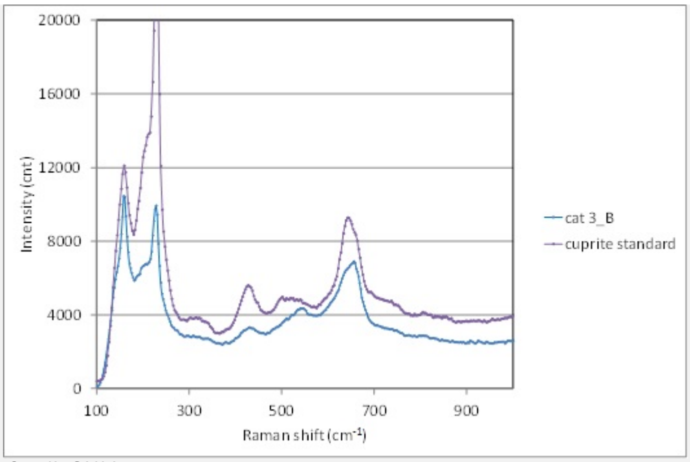

Credit SNM.

one accumulation, filter D2 (0.75-0.8 mW), hole 500, slit 80, grating 600. Method of analysis: Raman spectroscopy, Lab Swiss National Museum, Affoltern a. Albis ZH,

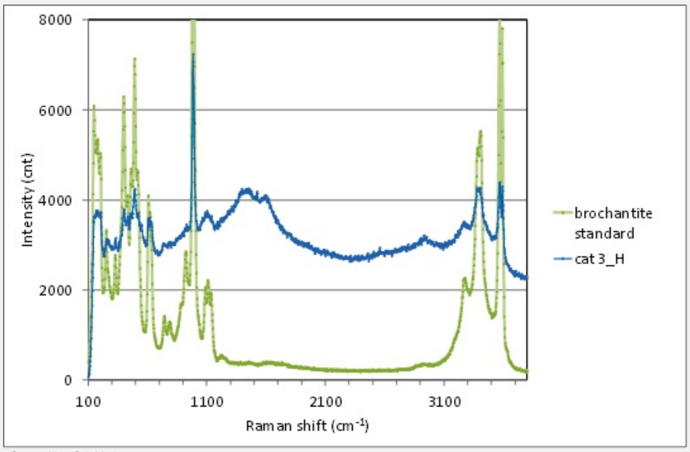

Credit SNM.

Fig. 10: Raman spectrum of the green outer corrosion layer (CP1) of the external side (cat3_H) compared to a brochantite standard spectrum. Settings: laser wavelength 532nm, acquisition time 100s, one accumulation, filter D2 (0.75-0.8 mW), hole 500, slit 80, grating 600. The peak indicated with an arrow on the cat3_H spectrum is due to fluorescence. Method of analysis: Raman spectroscopy, Lab Swiss National Museum, Affoltern a. Albis ZH,

Corrosion form	Uniform - pitting
Corrosion type	Type I (Robbiola)

Complementary information

Nothing to report.

MiCorr stratigraphy(ies) – CS

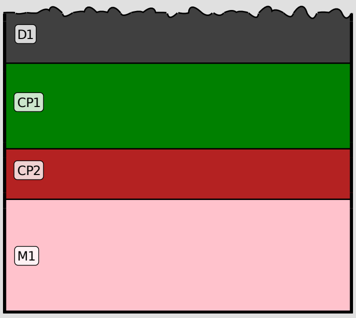

Fig. 4: Stratigraphic representation of the object in cross-section using the MiCorr application. This representation can be compared to Fig. 7.

Synthesis of the binocular / cross-section examination of the corrosion structure

Corrected stratigraphic representation: none.

Conclusion

The copper shingle was rolled (probably hot rolling) and annealed to recover the ductility of the original material. The metal is covered on its external side by a typical “urban outdoor” patina consisting of copper sulphate (brochantite/$Cu_4(OH)_6SO_4$) formed on top of a cuprite/Cu_2O layer. The surface of the internal side, protected from the diluted sulphuric acid present in urban rain water, has developed only a cuprite layer. The silica present in the brochantite on the external side is due to airborne particle pollution. The corrosion is probably of type 1 after Robbiola et al. 1998.

References

References on object and sample

1. Rapport d'analyse n° MAH 98-257. Laboratoire Musées d'art et d'histoire, Genève. The report describes a sample from another shingle.

References on analytic methods and interpretation

2. Robbiola, L., Blengino, J-M., Fiaud, C. (1998) Morphology and mechanisms of formation of natural patinas on archaeological Cu-Sn alloys, Corrosion Science, 40, 12, 2083-2111.
3. Selwyn, L. (2004) Metals and Corrosion: A Handbook for the Conservation Professional, Ottawa, ON: Canadian Conservation Institute, 68-70.
4. Stöckle, B., Mach, M. and Krätschmer, A. (1997) La durabilité des couvertures en cuivre selon les conditions environnementales. Résultat de l’UN/ECE-Programme d’exposition climatique, Les couvertures métalliques, matériaux et techniques, Les cahiers de la section française de l’ICOMOS, Paris, 129-135.
5. Welter, J-M. (2007) La couverture en cuivre en France: une promenade à travers les siècles, Le métal dans l’architecture, Monumental, 104-112.